Quasifission and fusion-fission in reactions with massive nuclei: Comparison of reactions leading to the $Z = 120$ element

A. K. Nasirov*
Joint Institute for Nuclear Research, Dubna, Russia

G. Giardina, G. Mandaglio, and M. Manganaro
Istituto Nazionale di Fizica Nucleare, Sezione di Catania, and Dipartimento di Fisica dell' Università di Messina, I-98166 Messina, Italy

F. Hanappe
Universit Libre de Bruxelles, 1050 Bruxelles, Belgium

S. Heinz and S. Hofmann
Gesellschaft für Schwerionenforschung, Darmstadt, Germany

A. I. Muminov
Institute of Nuclear Physics, Tashkent, Uzbekistan

W. Scheid
Institut für Theoretische Physik der Justus-Liebig-Universität, Giessen, Germany
(Received 21 December 2008; published 10 February 2009)

The yields of evaporation residues, fusion-fission, and quasifission fragments in the $^{48}Ca + ^{144,154}Sm$ and $^{16}O + ^{186}W$ reactions are analyzed in the framework of the combined theoretical method based on the dinuclear system concept and advanced statistical model. The measured yields of evaporation residues for the $^{48}Ca + ^{154}Sm$ reaction can be well reproduced. The measured yields of fission fragments are decomposed into contributions coming from fusion-fission, quasifission, and fast-fission. The decrease in the measured yield of quasifission fragments in $^{48}Ca + ^{154}Sm$ at the large collision energies and the lack of quasifission fragments in the $^{48}Ca + ^{144}Sm$ reaction are explained by the overlap in mass angle distributions of the quasifission and fusion-fission fragments. The investigation of the optimal conditions for the synthesis of the new element $Z = 120$ ($A = 302$) show that the $^{54}Cr + ^{248}Cm$ reaction is preferable in comparison with the $^{58}Fe + ^{244}Pu$ and $^{64}Ni + ^{238}U$ reactions because the excitation function of the evaporation residues of the former reaction is some orders of magnitude larger than that for the last two reactions.

DOI: 10.1103/PhysRevC.79.024606 PACS number(s): 25.70.Jj

I. INTRODUCTION

The observed evaporation residues in experiments are a result of the de-excitation of a heated and rotating compound nucleus formed in complete fusion reactions at heavy ion collisions. There are no evaporation residues if a compound nucleus is not formed. The correct estimation of the cross section of the compound nucleus formation in the reactions with massive nuclei is an important but difficult task. Different assumptions about the fusion process are used in different theoretical models and they can give different cross sections. The experimental methods used to estimate the fusion probability depend on the unambiguity of identification of the complete fusion reaction products among the quasifission products. The difficulties arise when the mass (charge) and angular distributions of the quasifission and fusion-fission fragments strongly overlap depending on the reaction dynamics. As a result, the complete fusion cross sections may be overestimated. We know that quasifission fragments show anisotropic angular distributions [1,2]. This is a way to separate them from the fusion-fission fragments that should have isotropic angular distributions. But fission fragments in reactions with heavy ions also show anisotropic angular distributions, which are explained by the assumption that an equilibrium K-distribution is not reached (K is the projection of the total spin of the compound nucleus on its axial symmetry axis). According to the transition state model [3,4] the formation of a compound nucleus with a large angular momentum leads to a large anisotropy A that is proportional to $\langle \ell^2 \rangle$:

$$A = 1 + \frac{\hbar^2 \langle \ell^2 \rangle}{4 J_{\rm eff} T_{\rm sad}}, \tag{1}$$

where

$$J_{\rm eff} = J_{\parallel} J_{\perp} / (J_{\perp} - J_{\parallel}) \tag{2}$$

is the effective moment of inertia of the compound nucleus on the saddle point; $J_{\parallel}$ and $J_{\perp}$ are moments of inertia around the axis of the axial symmetry and a perpendicular axis, respectively. $T_{\rm sad}$ is its effective temperature at the saddle point.

*Institute of Nuclear Physics, Tashkent, Uzbekistan; nasirov@jinr.ru.

At the same time the angular distribution of the quasifission fragments may be isotropic when the dinuclear system decays, having a large angular momentum [5].

This article is devoted to analyzing reasons for the lack or disappearance of the quasifission feature in the experimental data for the ^{48}Ca + ^{144}Sm and ^{48}Ca + ^{154}Sm reactions presented in the article by Knyazheva *et al.* [6], as well as to the comparison of the results for these reactions with the ones for the ^{16}O + ^{186}W reaction where there is no hindrance for complete fusion [6]. The same method of analysis is applied to study the problem of the synthesis of the new superheavy element $Z = 120$. The three reactions ^{54}Cr + ^{248}Cm, ^{58}Fe + ^{244}Pu, and ^{64}Ni + ^{238}U are compared with the aim of answering the question which of these reactions is preferable to obtain $Z = {}^{302}120$.

At first we consider the ^{48}Ca + ^{154}Sm reaction which shows evidently a yield of quasifission fragments at low energies. The results in detail were presented in Ref. [6]. According to the conclusion of the authors of this article the yield of quasifission fragments disappears by increasing the beam energy. The model of the dinuclear system predicts the presence of the quasifission features at large energies too [7–10]. Another interesting phenomenon is that the authors of Ref. [6] did not observe any yield of quasifission fragments in the ^{48}Ca + ^{144}Sm reaction, whereas in the present work we found a strong hindrance for the complete fusion in this reaction. The conclusions of the experimental investigation in Ref. [6] and our studies are in complete agreement for the very mass (charge) asymmetric ^{16}O + ^{186}W reaction: the hindrance to complete fusion is negligible. The results of the calculation of the above-mentioned phenomenon are discussed in Sec. II. In Sec. III, we present the results of estimating the evaporation residue yields to find the preferable reaction for the synthesis of the superheavy element $Z = 120$.

II. OVERLAPS OF THE FUSION-FISSION AND QUASIFISSION FRAGMENT DISTRIBUTIONS

All heavy ion reaction channels with the full momentum transfer at low collision energies take place through the stage of the dinuclear system (DNS) formation and can be called capture reactions. In the deep inelastic collisions DNS is formed but the full momentum transfer does not occur. Therefore, the deep inelastic collisions are not capture reactions. In the capture reactions the colliding nuclei are trapped into the well of the nucleus-nucleus potential after dissipation of part of the initial relative kinetic energy and orbital angular momentum. The lifetime of the DNS should be enough for its transformation into a compound nucleus during its evolution. The formation of the compound nucleus (CN) in reactions with massive nuclei has a hindrance: not all of the dinuclear systems formed at capture of the projectile by the target nucleus can be transformed into a CN. The decay of the DNS into two fragments bypassing the stage of the CN formation we call quasifission. The fast-fission process is the inevitable decay of the fast rotating mononucleus into two fragments without reaching the equilibrium compact shape of a CN. Such a mononucleus is formed from the dinuclear system that survived against quasifission. At large values of the angular momentum $\ell > \ell_f$, where ℓ_f is a value of ℓ at which the fission barrier of the corresponding compound nucleus disappears, the mononucleus immediately decays into two fragments [11]. As distinct from fast-fission, the quasifission can occur at all values of ℓ at which capture occurs.

In Ref. [6] the authors established the fusion suppression and the presence of quasifission for the reactions with the deformed ^{154}Sm target at energies near and below the Coulomb barrier. But the authors did not analyze the products with masses outside the range $55 < A < 145$. In the mass distribution of fission fragments from the ^{48}Ca + ^{154}Sm reaction they found an "asymmetric fission mode" appearing as "shoulders" peaked around the masses 65 and 140 at $E^*_{\rm CN} = 49$ and 57 MeV. Quasifission cross sections of this reaction have been extracted from the total fission-like events by the analysis of their mass and angular distributions. The analysis of these "asymmetric shoulders" in the mass energy distributions points to the quasifission nature of this component. The contribution of the quasifission fragments with masses in the above-mentioned range to the total mass distribution of fission fragments increases, with respect to one of the symmetric compound nucleus fission, as the ^{48}Ca projectile energy decreases. In Fig. 1(a) we compare the experimental

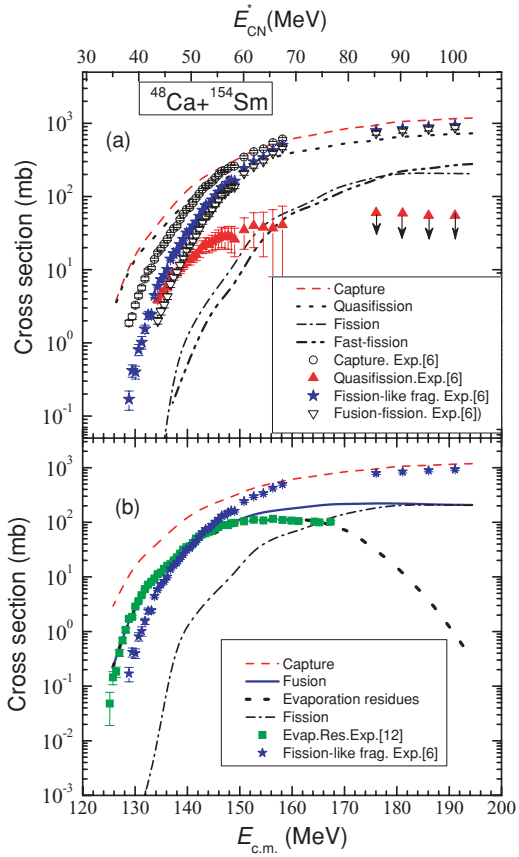

FIG. 1. (Color online) Comparison of the results of this work by the DNS model for the capture, complete fusion, quasifission, fast-fission, and evaporation residue cross sections with the measured data of the fusion-fission and quasifission given in Ref. [6] (panel (a)) and with data of the evaporation residues obtained from Ref. [12] (panel (b)) for the ^{48}Ca + ^{154}Sm reaction.

results for the capture, quasifission, and fusion-fission excitation functions from Ref. [6] presented with the results of calculations performed in the framework of the DNS model (see Refs. [13,14]). In this figure we present our results for the fast-fission fragments, too. The contribution of the fast-fission channel increases by increasing the bombarding energy due to the increase in the angular momentum of the mononucleus.

The origination of the measured fission-like fragments at the large bombarding energies is explained by the sum of the quasifission (short dashed line), fusion-fission (dash-double-dotted line), and fast-fission (dash-dotted line) fragments. At lower energies the contribution of the fusion-fission to the yield of binary fragments is small in comparison with the quasifission contribution. The small calculated fusion-fission cross section is explained by the large fission barrier ($B_f = 12.33$ MeV) for the ^{202}Pb nucleus according to the rotating finite range model by Sierk [15] and by the additional barrier $B_f^{(\text{microscopic})} = -\delta W = -(\delta W_{\text{saddle-point}} - \delta W_{\text{gs}}) \cong 8.22$ MeV caused by the nuclear shell structure. We conclude that the experimental fusion-fission data obtained at low energy collisions contain a huge contribution of quasifission fragments with masses $A > 83$ that show an isotropic distribution as presented in Ref. [6]. This is not a new phenomenon and it was discussed as a result of theoretical studies, for example, in our previous articles [16,17] and in Ref. [18]. The experimental results confirming this conclusion appeared recently in Refs. [19] and [20]. At the large energy $E_{\text{c.m.}} = 154$ MeV ($E^*_{\text{CN}} = 63$ MeV) the experimental values of the quasifission cross sections are much lower than those of the fusion-fission cross sections. A sufficient part of the quasifission fragments shows the behavior of the fusion-fission fragments: the mass distribution can reach the mass symmetric region and their angular distribution can be isotropic due to the possibility that the dinuclear system can rotate by large angles for large values of its angular momentum. The authors of Ref. [6] did not exclude such a behavior of the quasifission fragments. It is difficult to separate the quasifission fragments from the fusion-fission fragments when both their mass and angle distributions overlap in the region of symmetric masses.

It is well known that quasifission is the decay of the dinuclear system into two fragments with symmetric or asymmetric masses. The quasifission can take place at all values of the orbital angular momentum leading to capture. Quasifission fragments formed at energies above the Coulomb barrier with a small angular momentum contribute to the asymmetric part of the mass distribution. Because the lifetime of the dinuclear system decreases by increasing its excitation energy. The excitation energy is defined as

$$E^*_{\text{DNS}}(Z, A, \ell) = E_{\text{c.m.}} - V_{\min}(Z, A, \ell), \tag{3}$$

where $V_{\min}(Z, A, \ell)$ is the minimum of the potential well corresponding to the interaction of fragments with the charge (mass) asymmetry $\{Z, Z_{\text{tot}} - Z; A, A_{\text{tot}} - A\}$. As usual, the nucleus-nucleus potential $V(Z, A, \ell, R)$ includes the Coulomb $V_{\text{Coul}}(Z, A, R)$, nuclear $V_N(Z, A, R)$, and rotational $V_{\text{rot}}(Z, A, R, \ell)$ parts:

$$V(Z, A, \ell, R) = V_{\text{Coul}}(Z, A, R) + V_N(Z, A, R) + V_{\text{rot}}(Z, A, R, \ell), \tag{4}$$

where R is the distance between the centers of the nuclei. Details of the calculation can be found in Refs. [10] and [13].

At low energies the projectile-like quasifission fragments with $A < 70$ give a large contribution to the cross section for the considered ^{48}Ca + ^{154}Sm reaction because the excitation energy of the DNS is too small to shift the maximum of the mass distribution to the more mass symmetric configurations of the dinuclear system. The observed quasifission feature at low energies is connected with the peculiarities of the shell structure of the interacting nuclei. The increase in the beam energy leads to a decrease of the shell effects and the yield of the quasifission fragments near the asymmetric shoulders decreases. The main contribution to quasifission moves to the symmetric mass distribution. A more interesting phenomenon at the same beam energies occurs for the dinuclear system formed with large angular momenta. The lifetime of the DNS can be long enough to reach large rotational angles and to have a nearly isotropic angular distribution of its quasifission fragments because $E^*_{\text{DNS}}(Z, A, \ell)$ decreases as a function of angular momentum ℓ, according to its definition by Eq. (3). Of course, the quasifission barrier B_{qf} decreases by increasing ℓ but it decreases slower than $E^*_{\text{DNS}}(Z, A, \ell)$ because we have

$$|dE^*_{\text{DNS}}(Z, \ell)/d\ell| > |dB_{\text{qf}}/d\ell|, \tag{5}$$

i.e., $E^*_{\text{DNS}}(Z, \ell)$ decreases faster than B_{qf} by increasing ℓ (see Fig. 2) at all beam energies. This inequality follows from a comparison of the corresponding derivations that can be obtained using Eqs. (3) and (4):

$$\frac{dE^*_{\text{DNS}}(Z, \ell)}{d\ell} = -\frac{(2\ell + 1)\hbar^2}{2\left(J_1 + J_2 + \mu R^2_{\text{m}}\right)}. \tag{6}$$

Taking into account the definition of the quasifission barrier $B_{\text{qf}}(Z, \ell) = V_B(Z, \ell) - V_{\min}(Z, \ell)$ yields

$$\frac{dB_{\text{qf}}(Z, \ell)}{d\ell} = \frac{(2\ell + 1)\hbar^2}{2\left(J_1 + J_2 + \mu R^2_m\right)} - \frac{(2\ell + 1)\hbar^2}{2\left(J_1 + J_2 + \mu R^2_B\right)}, \tag{7}$$

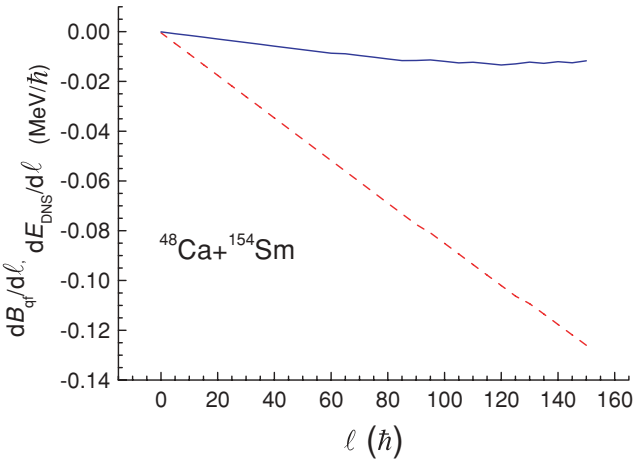

FIG. 2. (Color online) The decrease in the quasifission barrier $B_{\text{qf}}(Z, \ell)$ (solid line) and excitation energy $E^*_{\text{DNS}}(Z, \ell)$ (dashed line) of the dinuclear system as a function of the angular momentum for the ^{48}Ca + ^{154}Sm reaction.

where $V_B(Z, \ell)$ is the barrier of the nucleus-nucleus potential that should be overcome at the decay of the dinuclear system. $V_{\min}(Z, \ell)$ was discussed earlier; R_B and R_m are the positions of the barrier and minimum of the potential well with $R_B > R_m$. From a comparison of the right sides of Eqs. (6) and (7) we obtain Eq. (5). This inequality means that the dinuclear system can rotate by large angles before it decays into two fragments if it is formed with large angular momentum ℓ. A large beam energy is needed to form a dinuclear system with large values of ℓ. The condition is similar with the formation of superdeformed states of a nucleus. So, we can conclude that the quasifission fragments formed at the decay of the fast rotating dinuclear system have nearly isotropic angular distribution. If their mass distribution is in the region of symmetric masses then the quasifission fragments are very similar to the fusion-fission fragments and they are mixed with the latter. This mechanism is responsible for the disappearance of the "asymmetric shoulders" in the mass distribution of the fission fragments from the $^{48}\mathrm{Ca} + {}^{154}\mathrm{Sm}$ reactions at collision energies $E_{\mathrm{c.m.}} > 154$ ($E^*_{\mathrm{CN}} > 63$ MeV). The experimental data, which were identified as fusion-fission fragments by the authors of Ref. [6], increase strongly starting from the energies $E_{\mathrm{c.m.}} > 147$ ($E^*_{\mathrm{CN}} > 57$) MeV. According to our results, a large part of this increase belongs to the quasifission fragments (see Fig. 1). So we stress that, in the $^{48}\mathrm{Ca} + {}^{154}\mathrm{Sm}$ reaction, the quasifission [short dashed line in Fig. 1(a)] is the dominant channel in comparison with the fusion-fission (dash-dotted line), total evaporation residue [thick dotted line in Fig. 1(b)], and fast-fission [dashed-double dotted line in Fig. 1(a)] channels. The experimental data for the excitation function of the total evaporation residues are taken from the article by Stefanini *et al.* [12]. At energies $E_{\mathrm{c.m.}} < 140$ MeV, our capture cross section σ_{cap} overestimates the experimental values of the capture cross section $\sigma^{(\mathrm{exp})}_{\mathrm{cap}}$ because the authors of Ref. [6] excluded from their analysis the reaction products having mass numbers outside the mass range $55 < A < 145$. Our studies showed that capture events, i.e., events of the full momentum transfer, can lead to yields of fragments with masses $A_{\mathrm{qf}} < 55$. Consequently they lost a part of the capture cross sections related to the contributions of the quasifission fragments with $A_{\mathrm{qf}} < 55$. They determined

$$\sigma^{(\mathrm{exp})}_{\mathrm{cap}}(E_{\mathrm{c.m.}}, A_{\mathrm{qf}}) = \sigma^{(\mathrm{exp})}_{\mathrm{ER}}(E_{\mathrm{c.m.}}) + \sigma^{(\mathrm{exp})}_{f}(E_{\mathrm{c.m.}}) + \sigma^{(\mathrm{exp})}_{\mathrm{qf}}(E_{\mathrm{c.m.}}, 55 < A_{\mathrm{qf}} < 145), \quad (8)$$

while the theoretical capture cross section includes the contributions of all fragment yields, i.e., $4 < A_{\mathrm{qf}} < 198$, from full momentum tranfer reactions

$$\sigma_{\mathrm{cap}}(E_{\mathrm{c.m.}}) = \sigma_{\mathrm{ER}}(E_{\mathrm{c.m.}}) + \sigma_{\mathrm{f}}(E_{\mathrm{c.m.}}) + \sigma_{\mathrm{qf}}(E_{\mathrm{c.m.}}) + \sigma_{\mathrm{fast\,fission}}(E_{\mathrm{c.m.}}). \quad (9)$$

The experimental and theoretical capture cross sections come closer when the beam energy increases due to three main reasons: (i) a shift of the maximum of the DNS mass distribution to the mass symmetric region: the amount of the lost part of the capture cross section decreases; (ii) the quasifission fragments within the $70 < A_{\mathrm{qf}} < 130$ range that are formed at the decay of the DNS with large angular momentum show an isotropic angular distribution, being considered as fusion-fission fragments; (iii) the fusion probability increases by increasing the beam energy due to the inclusion of the contributions from collisions with large orientation angles of the target-nucleus symmetry axis (see Fig. 3) with respect to the beam direction. The favorableness of the large orientation angles for the formation of the compound nuclei was analyzed in Refs. [5,10,21]. This mechanism was earlier suggested by Ref. [22]. The probability of the compound nucleus formation P_{CN} increases by increasing the collision energy and the excitation energy E^*_{CN}, as seen in Fig. 3. The presented results in Figs. 1 and 3 are obtained by averaging over all orientation angles of the symmetry axis of ^{154}Sm, which is a well deformed nucleus ($\beta_2 = 0.341$). The role of the target orientation angle relative to the beam direction during the formation of the fusion-fission and ER products in the $^{48}\mathrm{Ca} + {}^{154}\mathrm{Sm}$ reaction was analyzed in Ref. [21]. The decrease in P_{CN} by increasing the DNS angular momentum ℓ is explained by the increase in the intrinsic fusion barrier and decrease in the quasifission barrier by increasing ℓ (see Refs. [13,14]). So, we have explained the large difference between the calculated and the experimental capture cross sections at low collision energies and the decrease in this difference at high collision energies. The experimental data of fission-like fragments seem to include some part of the quasifission and fast-fission fragments that overlaps with the mass and angular distributions of the fusion-fission fragments.

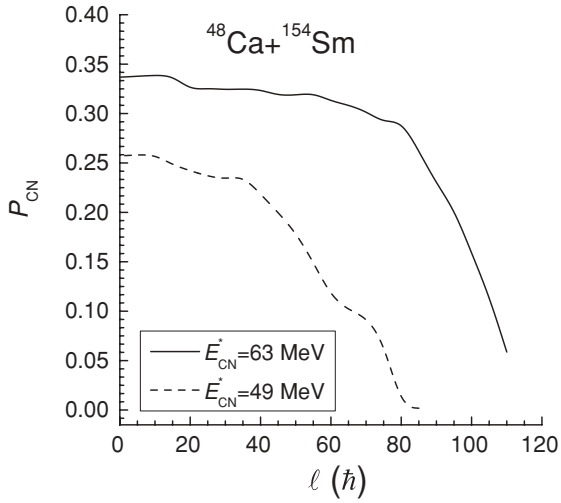

FIG. 3. The probability P_{CN} of the compound nucleus formation as a function of the angular momentum of the dinuclear system ℓ at energies $E_{\mathrm{c.m.}} = 138$ and 154 MeV, corresponding to the excitation energies of the compound nucleus $E^*_{\mathrm{CN}} = 49$ and 63 MeV, respectively.

The agreement of the results for the angular momentum distributions with the measured ones in Ref. [6] confirms that the angular momentum distributions of the compound nuclei obtained by us are correct. The results of this comparison are presented in Fig. 4. The deviation of the results for ℓ_{CN} of this work from the experimental data at $E_{\mathrm{c.m.}} = 138$ MeV is explained by large contributions of quasifission fragments.

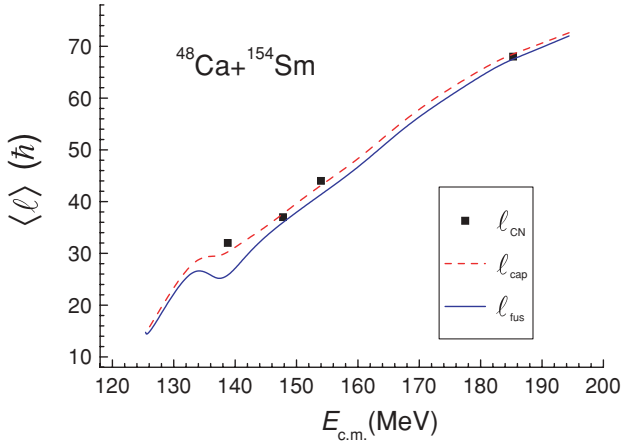

FIG. 4. (Color online) Comparison of the calculated angular momentum distribution of the compound nucleus ^{202}Pb formed in the ^{48}Ca + ^{154}Sm reaction with the experimental data from Ref. [6]. The presence of the quasifission contribution in the measured data is noticeable at low energies.

A. About missing quasifission events in the ^{48}Ca + ^{144}Sm reaction

The authors of Ref. [6] concluded from the study of mass angle distributions in ^{48}Ca + ^{144}Sm reactions that there are no quasifission contributions to the mass distribution in the analyzed range $60 < A < 130$. The theoretical calculations in this work show that quasifission occurs in this reaction causing the hindrance for the formation of the compound nucleus. But this hindrance is less active than the one in the case of the reaction with ^{154}Sm. The presence of the quasifission feature is expected from the nonzero value of the intrinsic fusion barrier B^*_{fus}, which is found from the driving potential calculated for the ^{48}Ca + ^{144}Sm reaction. The results for the capture, complete fusion, evaporation residue, fusion-fission and fast-fission cross sections are presented in Fig. 5. It is seen that the theoretical results indicate large contributions of quasifission to the capture cross section. Unfortunately, the authors of Ref. [6] did not investigate the fusion or evaporation residue cross sections that could be compared with our results. The contradiction between our results and the conclusion of the authors of Ref. [6] from their analysis of the selected experimental data about a presence or lack of quasifission in the ^{48}Ca + ^{144}Sm reaction may be removed if we answer the question why were the quasifission events not observed? There are two reasons: (i) one part of the mass distribution of the quasifission fragments is outside the analyzed range of $60 < A < 130$, and (ii) another part of the quasifission fragments is mixed with the fusion-fission fragments and has similar isotropic distributions. The masses of the missing quasifission fragments are in the mass range $48 < A < 60$. This range is outside the analyzed range and, therefore, the missing fragments cannot show the presence of quasifission. The isotope ^{144}Sm is a magic nucleus with neutron number $N = 82$. Therefore, the concentration of the asymmetric mode of the quasifission fragments in the mass range $48 < A < 60$ is explained by the effect of the shell structure of the double-magic projectile-nucleus ^{48}Ca and magic target-nucleus ^{144}Sm on the mass distribution of the reaction fragments. As a result the mass distributions of the products of deep inelastic collisions and asymmetric quasifission overlap in this mass range.

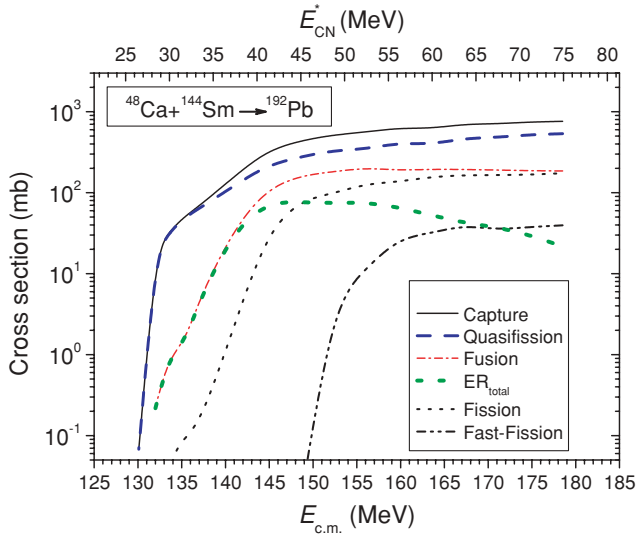

FIG. 5. (Color online) The results by the DNS model for the capture, complete fusion, quasifission, fission, evaporation residue, and fast-fission cross sections for the ^{48}Ca + ^{144}Sm reaction.

This case is similar to the ^{48}Ca + ^{208}Pb reaction where the presence of the quasifission feature was doubtful (see Ref. [9] and references therein). But our investigation showed that because of the collision of the double-magic ^{48}Ca and ^{208}Pb nuclei the mass distribution of the quasifission fragments is concentrated around the initial masses [9] because the potential energy surface has a local minimum in this region. Moreover the products of these processes have similar angular distributions for collisions with small values of the orbital angular momentum ℓ but they can be separated by the total kinetic energy distributions. In the quasifission process the full momentum transfer takes place. In collisions with large angular momentum the angular distributions of the products of the quasifission and deep inelastic collisions should be different because of the long lifetime of the dinuclear system formed at the capture stage of reaction. This kind of study will be useful to investigate the mechanism of the full momentum transfer reactions.

Concerning the second reason, the calculation of the mass distribution of quasifission fragments for the ^{48}Ca + ^{144}Sm reaction showed that there is another group of fragments that is placed in the mass symmetric region and is mixed with the fusion-fission fragments.

We suggest measuring the cross sections of the evaporation residues and comparing them with the corresponding data obtained in Ref. [12] for the ^{48}Ca + ^{154}Sm reaction. We expect that the excitation function of evaporation residues of the latter reaction will be higher than the one that could be obtained for the ^{48}Ca + ^{144}Sm reaction. This will be evidence for the presence of quasifission fragments in the ^{48}Ca + ^{144}Sm reaction. Of course, the fact that the compound nucleus ^{192}Pb formed in the last reaction has a smaller number of neutrons leads to a decrease in the evaporation residue cross sections but

the effect of quasifission should be stronger than the effect of the difference in the neutron numbers in the compound nuclei ^{192}Pb and ^{202}Pb. In Fig. 5 we present our theoretical results for the excitation function of the evaporation residues (thick short-dashed line) of the ^{48}Ca + ^{144}Sm reaction. A comparison of the results of σ_{ER} for the reactions with ^{154}Sm (see Fig. 1) and ^{144}Sm (Fig. 5) shows that the values of the former reaction are larger than the ones of the latter reaction. The fusion cross sections are nearly the same but the capture excitation function for the reaction with ^{144}Sm is lower than the one for the ^{48}Ca + ^{154}Sm reaction because the attractive nuclear forces are stronger in the more neutron rich system. So we can conclude that according to our theoretical studies there are quasifission events in the ^{48}Ca + ^{144}Sm reaction. The authors of Ref. [6] did not observe them because the mass distribution of the first group of quasifission fragments was outside the mass range $60 < A < 130$. The second group of the quasifission fragments has an overlap in the mass angle distributions with the fusion-fission fragments in the studied mass range.

B. About a lack of quasifission in the ^{16}O + ^{186}W reaction

To check the reliability of our calculation method we analyzed also the ^{16}O + ^{186}W reaction where the complete fusion is the main channel among capture reactions. Indeed, the driving potential of this reaction does not show an intrinsic fusion barrier $\ell = 0$ excluding a small barrier connected with the effect of the odd-even nucleon numbers. But an intrinsic fusion barrier can arise at large values of the orbital angular momentum ℓ. The results of the calculation for the capture, complete fusion, evaporation residue, and fusion-fission cross sections are presented in Fig. 6. One can see that up to $E_{c.m.} = 90$ MeV the excitation functions of capture and complete fusion are mainly the same because the contribution of quasifission is very small (more than one order lower). Certainly, the evaporation residue cross section is enough large and it decreases at large values of the beam energy due to the decrease in the stability of the heated and rotating compound

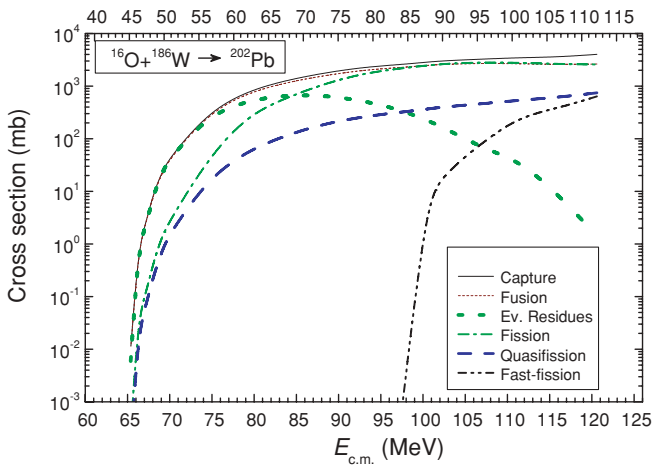

FIG. 6. (Color online) The results of the DNS model for the capture, complete fusion, quasifission, fission, evaporation residue, and fast-fission cross sections for the ^{16}O + ^{186}W reaction.

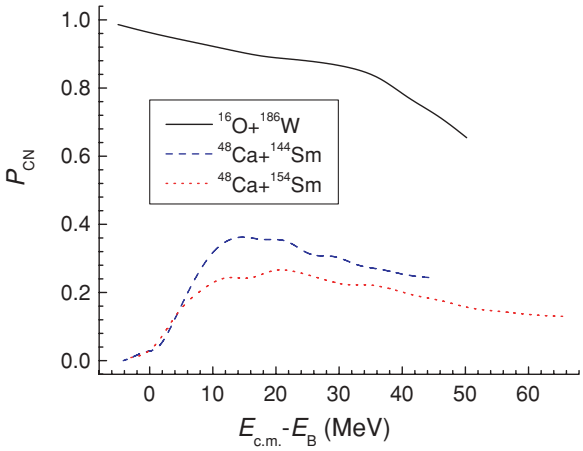

FIG. 7. (Color online) The DNS model results for the fusion probability P_{CN} for the ^{16}O + ^{186}W, ^{48}Ca + ^{144}Sm, and ^{48}Ca + ^{154}Sm reactions as a function of the collision energy relative to the interaction barriers corresponding to each of reactions.

nucleus. At $E_{c.m.} > 83$ MeV the fission cross section is higher than the ER cross section. The fast-fission contribution is small and it appears appreciably at $E_{c.m.} > 100$ MeV. The mass distribution of quasifission fragments does not reach the mass symmetric region and consequently there is not an overlap with fusion-fission fragments. The measured fission fragments correspond to a pure fusion-fission channel.

Concluding this section, in Fig. 7 we present the calculated fusion probability P_{CN} for the discussed reactions as a function of the collision energy relative to the corresponding interaction barrier for each reaction in the figure. It is seen that in the mass asymmetric ^{16}O + ^{186}W reaction the fusion probability is large. The mass distributions of quasifission fragments are near the target and projectile masses and they are not mixed with the fusion-fission fragments. Therefore, all fission fragments near the mass symmetric region belong to the fission of the compound nucleus. The quasifission process evidently takes place in the reactions ^{48}Ca + ^{144}Sm and ^{48}Ca + ^{154}Sm. It is more intense in the latter reaction. The lack of quasifission events in the experimental studies of the ^{48}Ca + ^{144}Sm reaction or the disappearance of quasifission events by increasing the beam energy is connected with the measurement and analysis of the experimental data. More advanced experimental methods can be developed to study the quasifission feature in the case where the mass angle distributions of the quasifission and fusion-fission fragments strongly overlap in the mass symmetric region.

III. ROLE OF THE CHARGE ASYMMETRY AND NUCLEAR SHELL STRUCTURE IN THE YIELDS OF REACTION PRODUCTS

The theoretical method based on the dinuclear system concept is used to analyze capture, complete fusion, quasifission, and fast-fission contributions in the reactions with massive nuclei and can be applied to estimate and make predictions of which of the reactions ^{54}Cr + ^{248}Cm, ^{58}Fe + ^{244}Pu, or

^{64}Ni + ^{238}U is most preferable to synthesize the superheavy element $Z = 120$.

The advantage of the cold fusion reactions is a large survival probability in the emission of one or two neutrons from the weak heated CN. This method was used to obtain the first superheavy elements $Z = 110$ (darmstadtium), 111 (roentgenium), 112 (see Refs. [23,24]), and 113 [25]. The grave disadvantage of "cold fusion" reactions is the dominance of the quasifission process as the channel causing a hindrance in transforming the DNS into a compound nucleus. According to the DNS model, for the more mass symmetric reactions, the intrinsic fusion barrier is larger in comparison with the one for mass asymmetric reactions [8,13,14]. But the hindrance caused by quasifission is not so strong in mass asymmetric "hot fusion" reactions. This is supported by the synthesis of the even heavier new elements $Z = 114$, 115, 116, and 118 that were observed in reactions with ^{48}Ca ion beams on ^{244}Pu, ^{243}Am, ^{245}Cm, and ^{249}Cf actinide targets at the Flerov Laboratory of Nuclear Reactions of JINR in Dubna [26,27]. The cross section for the synthesis of the new element 118 was about 0.5 pb in the ^{48}Ca + ^{249}Cf reaction [27]. The results of the calculations for the cross sections of formation of the dinuclear system, the compound nucleus, and evaporation residues in this reaction are presented in Fig. 8. The relatively good agreement between the experimental data and our estimations for the evaporation residues gives hope to use the method based on the dinuclear system concept to investigate which of the reactions ^{54}Cr + ^{248}Cm, ^{58}Fe + ^{244}Pu, or ^{64}Ni + ^{238}U is preferable to synthesize the superheavy element $Z = 120$.

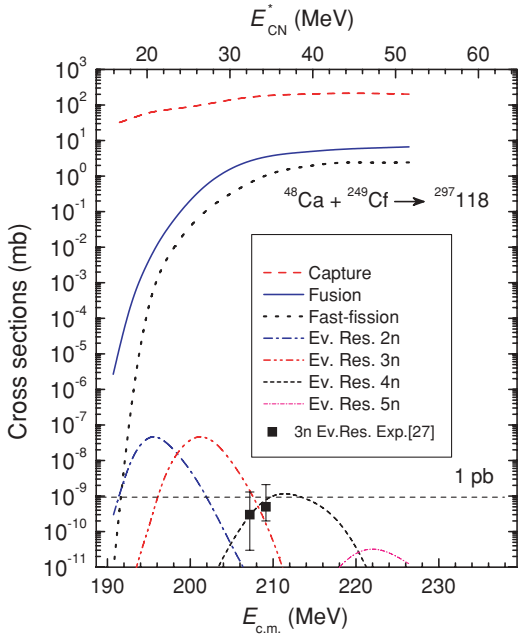

FIG. 8. (Color online) Excitation functions of the formation of the dinuclear system (capture), the compound nucleus (fusion), and fast-fission fragments in the ^{48}Ca + ^{249}Cf reaction (upper part of the figure). Comparison of the calculated evaporation residues in this reaction with the experimental data from Ref. [27] (lower part of the figure).

In Ref. [14], we discussed the difference in the yields of evaporation residues in different reactions leading to the same compound nucleus. It was shown that the relationship between the excitation energy E^*_{DNS} and the intrinsic barrier B^*_{fus} of the dinuclear system indicates which reaction is better at producing an evaporation residue with a large cross section. The results of the calculations in this work show that among the three reactions, ^{54}Cr + ^{248}Cm, ^{58}Fe + ^{244}Pu, and ^{64}Ni + ^{238}U, the first one is preferable for the synthesis of the superheavy element $Z = 120$ in comparison with the last two.

The analysis of the reactions with massive nuclei show that the mass asymmetry, shell structure, and orientation angles of the symmetry axes of the initial colliding nuclei play a crucial role in the formation of reaction products at the final stage of the process [5,8,13,14,21]. The failure in the synthesis of the superheavy element $Z = 118$ in the "cold fusion" reaction ^{86}Kr + ^{208}Pb at the Lawrence Berkeley Laboratory is explained by the very large value of B^*_{fus} of the dinuclear system consisting of the ^{86}Kr and ^{208}Pb nuclei. In other words, the touching point is far from the saddle point corresponding to the compound nucleus ^{294}118. Because of the small quasifission barrier the lifetime of the dinuclear system is short and its excitation energy is not sufficient to reach the saddle point. An increase of the beam energy does not supply the needed excitation energy because by increasing the beam energy the capture events are lost because of the smallness of the potential well in the nucleus-nucleus interaction between the nuclei. The calculated friction coefficient is not sufficient to trap the projectile into the small potential well at large energies. Details of this phenomenon are explained, for example, in Fig. 1 of Refs. [8] and [14] or Fig. 2 in Ref. [5]. The dynamics of the entrance channel was discussed in the last cited papers. This circumstance proves the importance of a correct calculation of the potential energy surface and the friction coefficients. Their quantities determine the distributions of the angular momentum and excitation energy between the fragments forming the DNS.

In the DNS model the capture and fusion stages are studied in detail to analyze experimental data. The observed hindrance to complete fusion in reactions with massive nuclei is connected with the intrinsic fusion barrier B^*_{fus} which is sensitive to the mass asymmetry and shell structure of the nuclei in the entrance channel [13,14]. The fusion barrier is determined by the peculiarities of the potential energy surface $U(Z, A, R)$ [13,14] calculated for the DNS leading to $Z = 120$ and $A = 302$. The potential energy surface is a sum of the mass balance for DNS fragments and the nucleus-nucleus interaction potential $V(Z, R)$:

$$U(Z, A, R) = B_1(Z) + B_2(Z_{tot} - Z) + V(Z, R) - B_{CN}(Z_{tot}), \quad (10)$$

where $B_1(Z)$, $B_2(Z_{tot} - Z)$, and $B_{CN}(Z_{tot})$ are the ground state binding energies of the DNS fragments 1 and 2 and the compound nucleus, respectively [13,14]. The potential energy surface, driving potential, and quasifission barriers for the reactions leading to the CN ^{302}120 are presented in Fig. 9. The characteristics of the entrance channel as mass (charge) asymmetry, shell structure, and orientation angles of

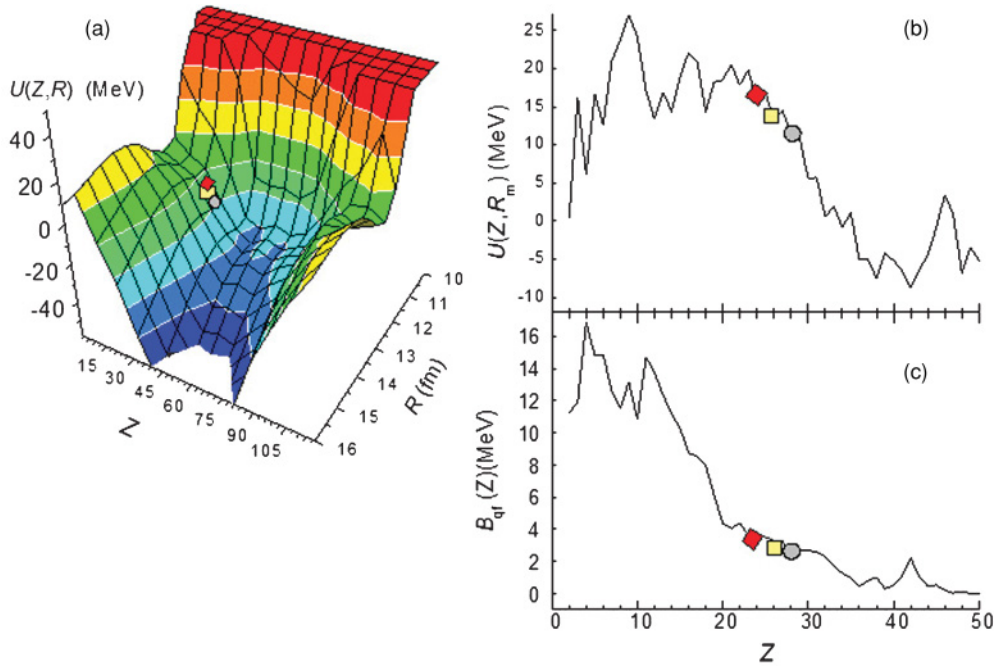

FIG. 9. (Color online) Potential energy surface $U(Z, R)$ calculated for the DNS configurations leading to the formation of the compound nucleus $Z = 120$ and $A = 302$ as a function of the fragment charge number Z and relative distance between the centers of fragments R (a), driving potential $U(Z, R_m)$ (b), and quasifission barriers $B_{\rm qf}$ as a function of Z (c). The initial points for the dinuclear systems formed in the ^{54}Cr + ^{248}Cm, ^{58}Fe + ^{244}Pu, and ^{64}Ni + ^{238}U reactions are shown by a diamond, a rectangle, and a circle, respectively.

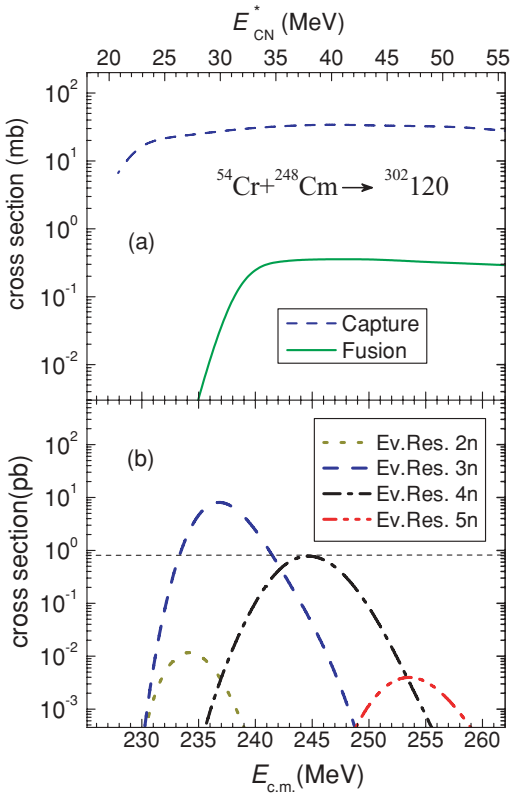

FIG. 10. (Color online) Calculated excitation functions for the capture and fusion (a) and for the formation of the evaporation residues in the $2n$, $3n$, $4n$, and $5n$ channels (b) in the the ^{54}Cr + ^{248}Cm reaction.

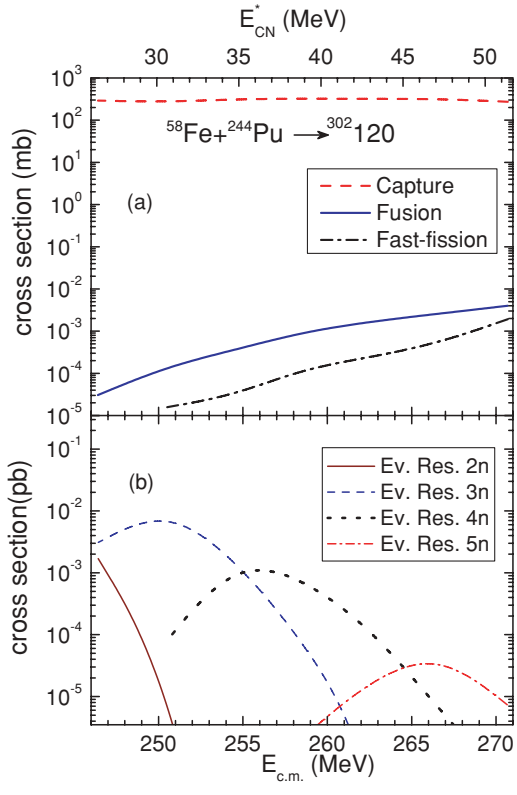

FIG. 11. (Color online) Calculated excitation functions for the capture, fusion, and fast-fission (a) and for the formation of the evaporation residues in the $2n, 3n, 4n$, and $5n$ channels (b) in the ^{58}Fe + ^{244}Pu reaction.

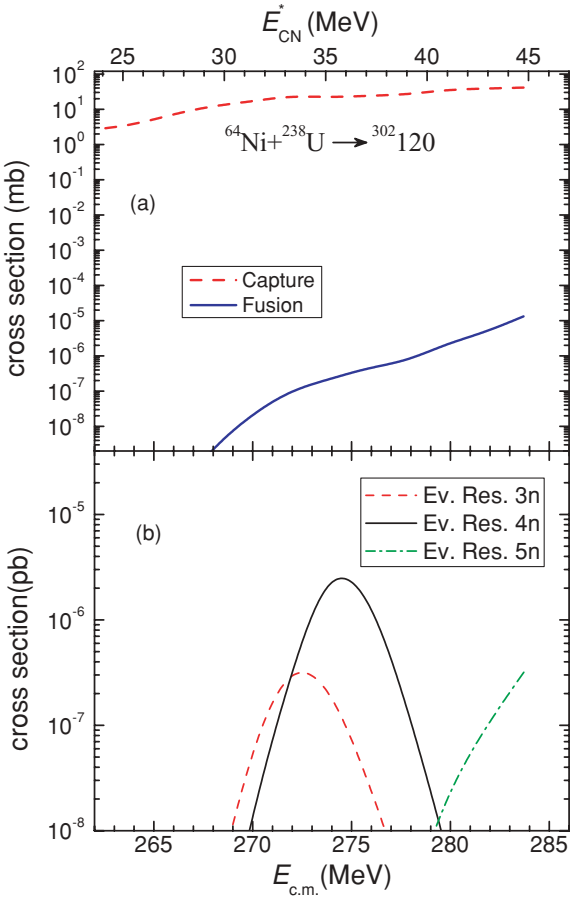

FIG. 12. (Color online) Calculated excitation functions for the capture and fusion (a) and for the formation of the evaporation residues in the $3n$, $4n$, and $5n$ channels (b) in the ^{64}Ni + ^{238}U reaction.

the symmetry axis (for the deformed nucleus) of colliding nuclei are important for the formation probability and angular momentum distribution of the compound nucleus. The survival probability of the heated and rotating compound nucleus depends on its angular momentum ℓ_{CN} and excitation energy E^*_{CN} [13,14]. The small intrinsic fusion barrier B^*_{fus} and large quasifission barrier B_{qf} lead to a large fusion probability. Figure 9 shows that the conditions are satisfied better for the ^{54}Cr + ^{248}Cm reaction.

It is seen from these figures that the ^{54}Cr + ^{248}Cm reaction is advantageous because it has the smallest intrinsic fusion barrier B_{fus}. The value of the potential energy for the DNS formed in this reaction at the capture stage is placed close to the maximum ("saddle point" to fusion) on the way to the fusion valley (to reach small values of Z) [Fig. 9(a)]. The quasifission barrier for this reaction is larger because it is more asymmetric in the charge (mass) than in the two other reactions [see Fig. 9(c)].

The results of the calculations of capture, complete fusion, and evaporation residue formation for the reactions ^{54}Cr + ^{248}Cm, ^{58}Fe + ^{244}Pu, and ^{64}Ni + ^{238}U are presented in Figs. 10, 11, and 12, respectively. We stress that the deformed shape of the initial projectile-target nuclei and the possibility of collisions with different orientation angles of their symmetry axes relative to the beam direction are taken into account as in Ref. [5]. The comparison of the Figs. 10, 11, and 12 shows that the ^{54}Cr + ^{248}Cm reaction is more favorable to synthesize the new superheavy element $Z = 120$ because the predicted excitation functions of the $3n$ and $4n$ evaporation residue channels are much larger than the maximal values for the other two reactions. We may state that the estimated evaporation residue cross sections are in the range of possibility of the detection systems used in the Flerov Laboratory of nuclear reactions of JINR (Dubna, Russia), SHIP of GSI (Darmstadt, Germany), and RIKEN (Japan).

IV. CONCLUSIONS

In this article we have analyzed the reasons for the missing of the quasifission features in the ^{48}Ca + ^{144}Sm reaction and the disappearance of the quasifission features in the ^{48}Ca + ^{154}Sm reaction at collision energies increasing from $E_{c.m.} = 154$ MeV to larger values in the experiments investigated in Ref. [6]. Our studies and analysis of complete fusion and formation of evaporation residues showed the presence of quasifission in both of these reactions. The experimental results for the capture, quasifission, and fusion-fission excitation functions from Ref. [6] and data on the evaporation residues for this reaction from Ref. [12] were compared with the results of calculations performed in the framework of the DNS model (see Refs. [13,14]). The appearance of the measured fission-like fragments at large bombarding energies is explained by the sum of the quasifission, fusion-fission, and fast-fission fragments. We conclude that the experimental fusion-fission data obtained at low collision energies contain a huge amount of contributions of quasifission fragments with masses $A > 83$ that show isotropic angular distributions as presented in Ref. [6]. The smallness of the calculated fusion-fission cross section is explained by the large fission barrier for the ^{202}Pb nucleus, $B_f = 12.33$ MeV, according to the rotating finite range model by Sierk [15] and the additional barrier $B_f^{(\text{microscopic})} \cong 8.22$ MeV caused by the nuclear shell structure. The quasifission fragments formed in the decay of the fast rotating dinuclear system have near isotropic angular distribution. Such fragments are mixed with the fusion-fission fragments if the mass distributions of both processes overlap in the region of symmetric masses. This mechanism is responsible for the disappearance of the "asymmetric shoulders" in the mass distribution of the fission fragments of the ^{48}Ca + ^{154}Sm reactions at collision energies $E_{c.m.} > 154$ ($E^*_{CN} > 63$ MeV). The experimental data, which were identified as fusion-fission fragments by the authors of Ref. [6], increase strongly starting from the energies $E_{c.m.} > 147$ ($E^*_{CN} > 57$) MeV. According to our results, a sufficient part of this increase belongs to the quasifission fragments (see Fig. 1). The calculated excitation function of the evaporation residues is in good agreement with the available experimental data from Ref. [12]. Its values for large collision energies decrease strongly due to the decrease in the fission barrier of the heated and rotating compound nucleus if its excitation energy and angular momentum increase.

The contradiction between our results and the conclusions of the authors of Ref. [6] from the analysis of the selected

experimental data about the lack of the quasifission process in the $^{48}Ca + ^{144}Sm$ reaction is connected by two main reasons: (i) the quasifission fragments have a mass distribution with the maximum outside of the analyzed range $60 < A < 130$; (ii) the quasifission fragments are mixed with the fusion-fission fragments and have similar isotropic distributions. The concentration of the first group of quasifission fragments in the mass range $48 < A < 60$ is explained by the effect of the shell structure of the double-magic projectile-nucleus ^{48}Ca and the magic target-nucleus ^{144}Sm on the mass distribution of the reaction fragments. Therefore, the mass distributions of the products from deep inelastic collisions and quasifission overlap in this mass range. A similar case was analyzed for the $^{48}Ca + ^{208}Pb$ reaction in Ref. [9]. Products of the decay of the long-lived dinuclear system that were formed at large values of the angular momentum contributing to the mass range $60 < A < 130$ seemed to be considered as the products of the fusion-fission reactions because the products of both processes have overlap of the mass and angular distributions.

The results obtained for the $^{16}O + ^{186}W$ reaction show that a hindrance for complete fusion [6] is negligible. Using the experience obtained in the analysis of the above-mentioned reactions we estimate the most preferable reaction for the synthesis of the superheavy element $Z = 120$. Among the three studied reactions, $^{54}Cr + ^{248}Cm$, $^{58}Fe + ^{244}Pu$, and $^{64}Ni + ^{238}U$, the first one is most preferable for the synthesis of the element $Z = 120$. Because it is a more asymmetric reaction having a smaller intrinsic fusion barrier and a larger quasifission barrier. These lead to a larger fusion cross section. The expected cross section for the synthesis of superheavy element $Z = 120$ in the $^{54}Cr + ^{248}Cm$ reaction is more than 1 pb for the $3n$ evaporation channel and about 1 pb the maximal value for the $4n$ channel in the $E_{c.m.} = 233$–245 MeV energy range.

ACKNOWLEDGMENTS

A.K.N. is grateful to the SHIP group in GSI and the Physics Department of the Messina University for warm hospitality during his stay. This work was performed partially under the financial support of the DFG, the RFBR, and the INTAS, which are thanked by A.K.N. A.K.N. and G.G. are also grateful to the Fondazione Bonino-Pulejo of Messina for the support received in the Collaboration between the Dubna and Messina groups.

[1] J. Tõke, R. Bock, G. X. Dai, A. Gobbi, S. Gralla, K. D. Hildenbrand, J. Kuzminski, W. F. J. Müller, A. Olmi, and H. Stelzer, Nucl. Phys. **A440**, 327 (1985).
[2] W. Q. Shen, J. Albinski, A. Gobbi, S. Gralla, K. D. Hildenbrand, N. Herrmann, J. Kuzminski, W. F. J. Müller, H. Stelzer, J. Tõke, B. B. Back, S. Bjornholm, and S. P. Sorensen, Phys. Rev. C **36**, 115 (1987).
[3] I. Halpern and V. M. Strutinski, in *Proceedings of the Second United Nations International Conference on the Peaceful Uses of Atomic Energy, Geneva, 1958* (United Nations, Geneva, 1958), Vol. 15, p. 408.
[4] J. J. Griffin, Phys. Rev. **116**, 107 (1959).
[5] A. K. Nasirov, A. I. Muminov, R. K. Utamuratov, G. Fazio, G. Giardina, F. Hanappe, G. Mandaglio, M. Manganaro, and W. Scheid, Eur. Phys. J. A **34**, 325 (2007).
[6] G. N. Knyazheva, E. M. Kozulin, R. N. Sagaidak, A. Yu. Chizhov, M. G. Itkis, N. A. Kondratiev, V. M. Voskressensky, A. M. Stefanini, B. R. Behera, L. Corradi, E. Fioretto, A. Gadea, A. Latina, S. Szilner, M. Trotta, S. Beghini, G. Montagnoli, F. Scarlassara, F. Haas, N. Rowley, P. R. S. Gomes, and A. Szanto de Toledo, Phys. Rev. C **75**, 064602 (2007).
[7] G. Giardina, F. Hanappe, A. I. Muminov, A. K. Nasirov, and L. Stuttgè, Nucl. Phys. **A671**, 165 (2000).
[8] G. Giardina, S. Hofmann, A. I. Muminov, and A. K. Nasirov, Eur. Phys. J. A **8**, 205 (2000).
[9] G. Fazio, G. Giardina, G. Mandaglio, F. Hanappe, A. I. Muminov, A. K. Nasirov, W. Scheid, and L. Stuttgé, Mod. Phys. Lett. A **20**, 391 (2005).
[10] A. Nasirov, A. Fukushima, Y. Toyoshima, Y. Aritomo, A. Muminov, Sh. Kalandarov, and R. Utamuratov, Nucl. Phys. **A759**, 342 (2005).
[11] C. Gregoire, C. Ngo, E. Tomasi, B. Remaud, and F. Scheuter, Nucl. Phys. **A387**, 37c (1982).
[12] A. M. Stefanini *et al.*, Eur. Phys. J. A **23**, 473 (2005).
[13] G. Fazio, G. Giardina, A. Lamberto, R. Ruggeri, C. Saccà, R. Palamara, A. I. Muminov, A. K. Nasirov, U. T. Yakhshiev, and F. Hanappe, Eur. Phys. J. A **19**, 89 (2004).
[14] G. Fazio, G. Giardina, G. Mandaglio, R. Ruggeri, A. I. Muminov, A. K. Nasirov, Yu. Ts. Oganessian, A. G. Popeko, R. N. Sagaidak, A. V. Yeremin, S. Hofmann, F. Hanappe, and C. Stodel, Phys. Rev. C **72**, 064614 (2005).
[15] A. J. Sierk, Phys. Rev. C **33**, 2039 (1986).
[16] G. Fazio, G. Giardina, A. Lamberto, R. Ruggeri, F. Hanappe, T. Materna, U. Yu. Jovliev, A. V. Khugaev, A. I. Muminov, and A. K. Nasirov, in *Proceedings of the International Symposium New Projects and Lines of Research in Nuclear Physics, Messina, Italy, 24–26 October 2002*, edited by G. Fazio and F. Hanappe (World Scientific, Singapore, 2003), pp. 258–271.
[17] A. K. Nasirov, G. Giardina, A. I. Muminov, W. Scheid, and U. T. Yakhshiev, in *Proceedings of the Symposium Nuclear Clusters, Rauischholzhausen, Germany, 5–9 August 2002*, edited by R. V. Jolos and W. Scheid (EP Systema, Debrecen, 2003), pp. 415–426; Acta Phys. Hung. A **19**, 109 (2004).
[18] Y. Aritomo and M. Ohta, Nucl. Phys. **A744**, 3 (2004).
[19] D. J. Hinde, R. du Rietz, M. Dasgupta, R. G. Thomas, and L. R. Gasques, Phys. Rev. Lett. **101**, 092701 (2008).
[20] G. N. Knyazheva, M. G. Itkis, E. M. Kozulin, V. G. Lyapin, V. A. Rubchenya, W. Trzaska, and S. V. Khlebnikov, Part. Nucl. Lett. **5**, No. 1 (143), 40 (2008) (in Russian).
[21] G. Fazio, G. Giardina, F. Hanappe, G. Mandaglio, M. Manganaro, A. I. Muminov, A. K. Nasirov, and C. Saccá, J. Phys. Soc. Jpn. **77**, 124201 (2008).
[22] D. J. Hinde, M. Dasgupta, J. R. Leigh, J. P. Lestone, J. C. Mein, C. R. Morton, J. O. Newton, and H. Timmers, Phys. Rev. Lett. **74**, 1295 (1995).
[23] S. Hofmann and G. Munzenberg, Rev. Mod. Phys. **72**, 733 (2000).
[24] K. Morita *et al.*, J. Phys. Soc. Jpn. **73**, 2593 (2004).
[25] K. Morita *et al.*, J. Phys. Soc. Jpn. **76**, 043201 (2007).
[26] Yu. Ts. Oganessian *et al.*, Phys. Rev. C **70**, 064609 (2004).
[27] Yu. Ts. Oganessian *et al.*, Phys. Rev. C **74**, 044602 (2006).